


Article

# Transition Analysis and Its Application to Global Path Determination for a Biped Climbing Robot

Haifei Zhu <sup>1</sup> , Shichao Gu <sup>1</sup>, Li He <sup>1</sup>, Yisheng Guan <sup>1,\*</sup> and Hong Zhang <sup>1,2</sup>

<sup>1</sup> School of Electromechanical Engineering, Guangdong University of Technology, Guangzhou 510006, China; hfzhu@gdut.edu.cn (H.Z.); xuguqian9@163.com (S.G.); heli@gdut.edu.cn (L.H.); hzhang@ualberta.ca (H.Z.)

<sup>2</sup> Department of Computing Science, University of Alberta, Edmonton, AB T6G2H1, Canada

\* Correspondence: ysguan@gdut.edu.cn; Tel.: +86-20-3932-2212

Received: 26 December 2017; Accepted: 11 January 2018; Published: 16 January 2018

**Abstract:** Biped climbing robots are considered good assistants and (or) substitutes for human workers carrying out high-rise truss-associated routine tasks. Flexible locomotion on three-dimensional complex trusses is a fundamental skill for these robots. In particular, the capability to transit from one structural member to another is paramount for switching objects to be climbed upon. In this paper, we study member-to-member transition and its utility in global path searching for biped climbing robots. To compute operational regions for transition, hierarchical inspection of safety, reachability, and accessibility of grips is taken into account. A novel global path rapid determination approach is subsequently proposed based on the transition analysis. This scheme is efficient for finding feasible routes with respect to the overall structural environment, which also benefits the subsequent grip and motion planning. Simulations are conducted with Climbot, our self-developed biped climbing robot, to verify the efficiency of the presented method. Results show that our proposed method is able to accurately determine the operational region for transition within tens of milliseconds and can obtain global paths within seconds in general.

**Keywords:** transition analysis; global path determination; path planning; biped climbing robot; truss-climbing robot

## 1. Introduction

Trusses typically comprise a number of triangular units constructed with straight rigid members whose ends are connected through joints. In modern architecture, spatial trusses are widely used in the construction of roofs, towers, bridges, and the like. Celebrated buildings include, for example, the Bird's Nest Stadium in Beijing, the Eiffel Tower in Paris, and the Auckland Harbor Bridge. Besides, scaffolds on which workers process the exterior of buildings are also typical spatial trusses. At present, truss-associated routine tasks such as construction, painting, inspection, maintenance, and so on, rely highly on manual labor, signifying a great risk to workers' safety.

Robots are ideal assistants or substitutes for human workers carrying out these high-rise and high-intensity tasks. In the past decades, a number of robots have been developed for climbing on trusses or truss members, including, SM<sup>2</sup> [1], ROMA [2], the brachiating robot [3], TREPA [4,5], WOODY [6,7], Shady3D [8], RiSE [9,10], UT-PCR [11], 3DCLIMBER [12], Treebot [13], the tendril-based bio-inspired robot [14], Climbot [15,16], and the Snake Robot [17]. Configuring different locomotion and attaching mechanisms, these robots differ significantly in mobility and flexibility. In-depth discussions on this topic could be found in [18,19]. Among these robots, SM<sup>2</sup>, ROMA, Shady3D, 3DCLIMBER, Treebot and Climbot, having the characteristic of bipedal climbing, are considered to be dominant. These biped climbing robots (BiCRs) generally comprise of an arm-like serial body for locomotion and grippers at both ends for attachment. Benefiting from the bipedal climbing patterns

inspired by arboreal primates [20], BiCRs have the flexibility to imitate transition between branches, as illustrated in Figure 1. This transition capability is paramount for robots switching objects to be climbed upon, especially for executing tasks on large-scale spatial complex structures. Another distinct advantage of BiCRs is the combination of manipulation and mobility. Hence, BiCRs are also known as mobile manipulators [1,15]. As a featured example, SM<sup>2</sup> was designed to work on the truss and other exterior surfaces of the Space Station Freedom for performing routine tasks. Besides, the two underactuated miniature climbing robots in [21], MATS [22], Frambot [23] and W-Climbot [24] are also typical BiCRs. Although coupled climbing robots have been developed in the past, most research focused on the system prototype and experimental verification of climbing patterns on simple structures [25,26]. Few attention in the literature has been paid to the perception and planning of this type of robots when traveling in truss environments. In this paper, we study the BiCR climbing path planning problem.

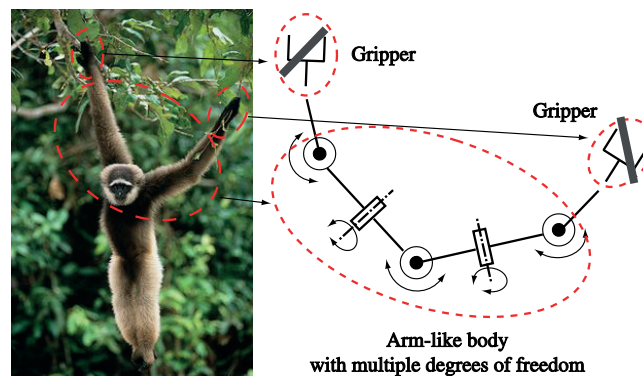


Figure 1. The inspiration for biped climbing robots.

Routine truss-associated tasks usually involve the transition from one member to another. Therefore, the transition issue must be handled well before looking into the climbing path planning problem. BiCR transit was qualitatively described in [2,27,28], but neither quantitative analysis nor executable output can be found in detail. In [29], a BiCR with five degrees of freedom (DoF) was proven capable of transiting between two cylindrical members at any relative orientation. Unfortunately, the distance of the members was not considered in this paper, and it was assumed that the robot could always reach its target member at any time. This is not the case in real situations. Moreover, the issue of where and how to transit was not dealt with, preventing the transition from practice. In [30,31], approaches for determining the graspable region in a climbing cycle were presented. The resulting graspable region, however, corresponds to a fixed grip only, i.e., one end attached at a known point. Theoretically, the entire operational region for transition could be numerically obtained by sampling the gripping point on both members alternatively, solving the graspable region for each and then merging all regions. Despite probabilistic completeness, this is intensive in terms of time and computational resources.

Lacking a close-formed solution for transition analysis, concrete transiting motion is always ignored in studies of path planning on trusses. Hierarchical control structure and multi-phase control strategy were discussed in [32], where only the truss junctions were considered attachable by SM<sup>2</sup>. Additionally, the initial and final states of the robot's two feet for each climbing cycle were artificially designated. In other words, neither path planning nor member-to-member transition were required by SM<sup>2</sup>. In [2], the path planning of ROMA, a robot designed for inspection applications in 3D environments, was modeled as a classical traveling salesman problem (TSP), taking a climbing step as the smallest unit for the consideration of energy cost. The TSP was finally solved by optimizing the energy consumption. However, only the middle and both ends of a member are allowed to attach for the robot. Similar research was done in [28], with a stricter calculation of the energy consumed in terms of a specific climbing gait. One obvious but important issue in both [2,28] is that the ability

of a gripper to grip a member on the expected point was neglected. In the real world, the spatial relationships of gripper fingers and members must be properly considered. Otherwise, the robot may fail in attachment, and thereby fall down. This issue was well handled in [27] by defining a node with its position, direction, and face on a truss. Truss members were dispersed into a number of limited nodes, each representing a discrete gripping point (The term “gripping point” used in this paper consists of the position vector and the orientation matrix to locate a grip in 3D space.). The best path to a destination on the truss was then determined by optimizing the path length and the cost of difficult maneuvers. However, owing to the limitation in locomotion flexibility, Shady3D has only one type of climbing gait, and performs simple transition within a plane cooperating with another unit. Consequently, the path planning of Shady3D robots is simpler than that of a more flexible BiCR with greater DoF. To assemble a truss with multiple Shady3D robots, the truss navigation problem was investigated in [33], where each Shady3D was treated as a single movable point. The trunks and branches of trees form natural truss structures upon which the path planning problem was studied in [34]. A grid map with bottom-up rings comprised by discrete points was used to model the surfaces of the trunk and branch. A sequence of gripping points was afterwards arranged by considering the motion cost, gravity, robot orientation, and its reachability. This method is applicable to climbing robots with nonenclosure gripping, i.e., Treebot, as stated in the paper, but not to BiCRs, such as SM<sup>2</sup> and Climbot, which use enclosure gripping and can flip over the head and tail in climbing. In a word, to the best of our knowledge, few efforts have been made in the field of BiCR path planning on three-dimensional (3D) complex trusses, while complete transition analysis has not yet been reported.

Our Climbot, originally developed in 2007 [15], is a robot designed to carry out high-rise routine tasks. Figure 2 shows the latest version of Climbot and its kinematic diagram. Compared with other BiCRs, Climbot has more climbing gaits and a stronger ability to negotiate obstacles and transit between structural members owing to its agile body and control, transplanted from powerful and light-weight industrial robots.

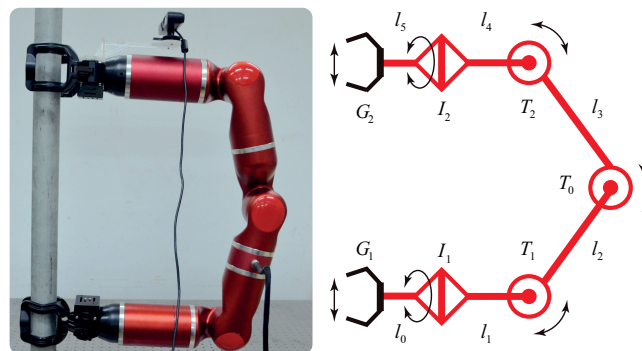


**Figure 2.** Climbot and its kinematic diagram.

To address the path planning problem of BiCRs in 3D complex truss environments, firstly, we propose a theoretical analysis of the transition between any two given members. The principle of transition analysis was previously presented in [35], and will be further improved by considering the grip accessibility in this paper. As far as we know, our proposed algorithm is the only one capable of determining both the possibility and operational regions for transition in tens of microseconds, considering the safety, reachability, and accessibility of grips. Secondly, we propose a novel path planning algorithm based on transition analysis, for a rapid generation of all feasible global paths on trusses from a start point to the given destination.

The remainder of this paper is organized as follows. We firstly introduce global path planning and transition problems of BiCRs in Section 2. We then analyze the transition requirements and constraints to compute the operational region in Section 3. We apply the transition analysis to fast determination of global climbing paths, with algorithm implementations presented in Section 4. In Section 5, we conduct

simulations with Climbot to verify the proposed analysis and algorithms. Finally, we conclude our work in Section 6.

## 2. Problem Statement

### 2.1. Global Path for Traveling on Trusses

For BiCRs moving on trusses, path planning determines a sequence of discrete gripping points along the way from the original point to the destination, and the corresponding collision-free motions transfer the moving end from one gripping point to another. On a universal 3D complex truss, step-by-step blind exploration is very time- and resource-consuming, resulting in extremely low searching efficiency. In addition, the increase in the number of members will greatly reduce the efficiency of path searching. Global guidance, as a promising solution, is hence important and necessary to avoid inefficient searching. Unlike the path planning problems on 2D or 2.5D terrain, where providing the gradient from the original point to the destination may be sufficient, efficient global guidance for BiCRs traveling on trusses must indicate the entire path, member by member, as shown in Figure 3. Operational regions for performing transition between each pair of members must also be provided, in order to facilitate the subsequent grip planning.

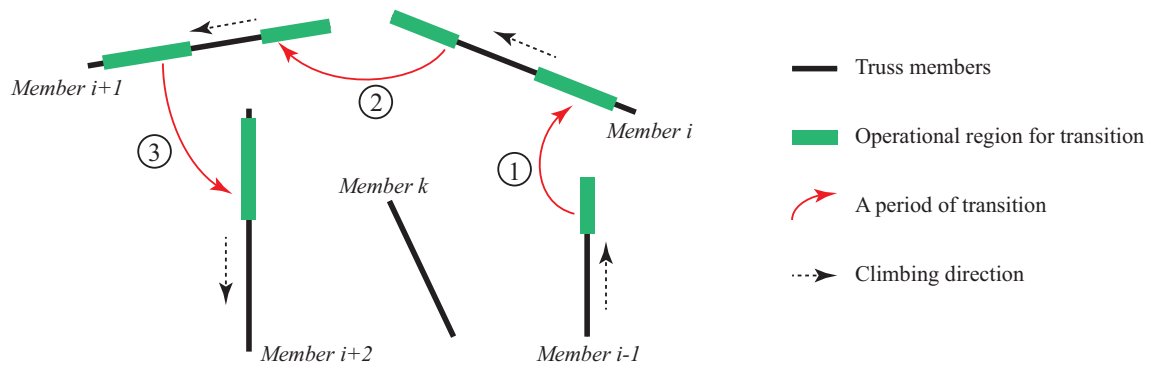


**Figure 3.** An illustration of global path for BiCRs traveling on a truss.

Since the crucial point of global path planning is to provide global guidance for the subsequent processes, it does not require details such as where to grip and how to move during each climbing cycle, but concentrates on the fast determination of feasible routes based on the overall structural environment. It should be underlined that these feasible routes will be discarded if later processing fails. However, the distinguishing merit is that the searching space is largely narrowed down to a limited number of members with step-by-step guidance by the so-called global path planner. As a result, the searching efficiency is expected to be largely increased.

### 2.2. Transition from One Member to Another

Operational regions for transition are the junction of a route. Therefore, transition analysis plays a fundamental role in global path planning on trusses. However, transition analysis for BiCRs is challenging due to many constraints, such as robot kinematics, geometries of members, and gripper features.

Basically, a BiPCR performing a transition from Member 1 to Member 2 is illustrated in Figure 4 and is described below, supposing the robot originally grips on Member 1 at the beginning.

- The robot starts to move its end effector, i.e., the swinging gripper, towards Member 2, as indicated in Figure 4a.
- After aligning well with Member 2, the robot shifts its swinging gripper to the desired gripping point, as shown in Figure 4b.

- (c) The robot grips on *Member 2* with its swinging gripper and holds the two members at the same time, as shown in Figure 4c.
- (d) The robot releases the base gripper from *Member 1*. Afterwards the two grippers alternate their roles.
- (e) The new swinging gripper moves away from *Member 1*, then towards its new target gripping point. Procedures (d) and (e) correspond to Figure 4d.

Accordingly, a valid transition has the following requirements.

- Safety. The robot must be able to support itself reliably with only one grip, as required in phases (a)–(e), respectively.
- Reachability. The robot must be able to simultaneously grip both members with its two grippers, satisfying kinematic constraints, as illustrated in phase (c).
- Accessibility. Grips on both members must be accessible by corresponding grippers, as required in phases (b) and (e). Each grip’s accessibility must be considered in two aspects: when the gripper moves towards the grip, and when the gripper moves away from the grip after alternating its role. Considering the 3/4 envelope pattern used, possibilities for the gripper moving forwards and backwards with respect to a grip in the gripping direction for a specified safe distance, are accounted the corresponding grip’s accessibility.

These three criteria form the basis for transition analysis. Regarding safety checks, strict computation considering dynamics is neither necessary nor practical at the global path planning stage, which will be discussed later on. For reachability and accessibility inspection we propose a mathematical model for further analysis.

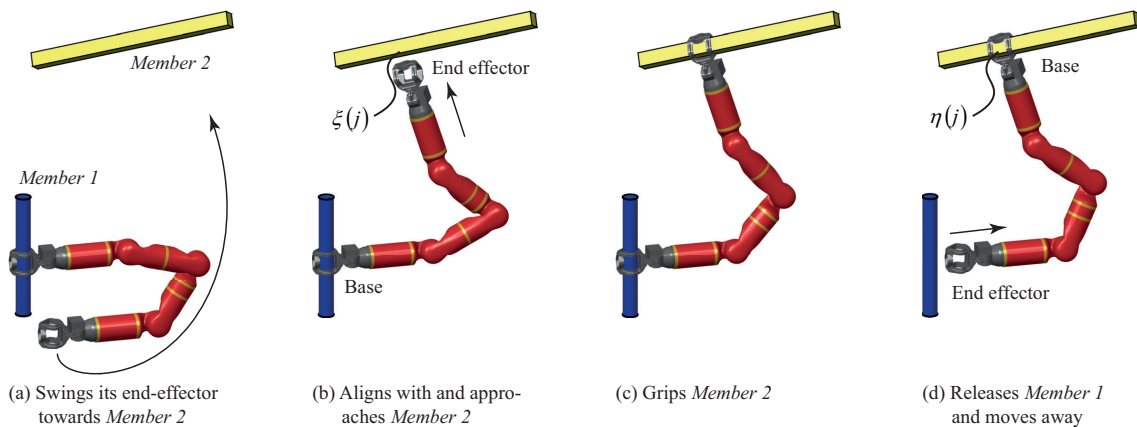


**Figure 4.** Procedures in the transition from *Member 1* to *Member 2*, illustrated with Climbot.

Without loss of generality, the transition problem can be depicted as a geometric model, as shown in Figure 5. Denote  $\{W\}$  as the world coordination frame, and arrange  $\{U\}$ ,  $\{V\}$ ,  $\{B\}$  and  $\{E\}$  to the reference points of two members, the current and target gripping points, respectively. We use parametric equations to express the gripping positions and transformation matrices to represent grips for BiCRs. Considering reachability and accessibility, we have the following problem statement:

- Given:
- ${}^W_B \mathbf{P} = {}^W_U \mathbf{P} + t_1 {}^W \mathbf{d}_1$  Points on *Member 1*
  - ${}^W_E \mathbf{P} = {}^W_V \mathbf{P} + t_2 {}^W \mathbf{d}_2$  Points on *Member 2*
  - ${}^W_U \mathbf{R}$  Current gripping orientation
  - ${}^W_V \mathbf{R}$  Goal gripping orientation
  - $\mathbf{q} = IK({}^B_E \mathbf{T})$  Robot inverse kinematics
- To solve:  $t_1$  and  $t_2$  Operational regions for transition satisfying Equations (1) to (4)

$${}^W_B \mathbf{T} = \begin{bmatrix} {}^W_U \mathbf{R} & {}^W_B \mathbf{P} \\ \mathbf{0} & 1 \end{bmatrix}, \quad {}^W_E \mathbf{T} = \begin{bmatrix} {}^W_V \mathbf{R} & {}^W_E \mathbf{P} \\ \mathbf{0} & 1 \end{bmatrix}, \quad (1)$$

$$\exists \mathbf{q} = IK(\mathop{\mathrm{W}}{\mathrm{T}}_B^{-1} \mathop{\mathrm{W}}{\mathrm{T}}_E), \tag{2}$$

$$\exists \mathbf{q} = IK(\mathop{\mathrm{W}}{\mathrm{T}}_B^{-1} \mathop{\mathrm{W}}{\mathrm{T}}_E \mathop{\mathrm{E}}{\mathrm{T}}_{E'}), \tag{3}$$

$$\exists \mathbf{q} = IK(\mathop{\mathrm{R}}_{RxE} \mathop{\mathrm{W}}{\mathrm{T}}_B^{-1} \mathop{\mathrm{W}}{\mathrm{T}}_{B'} \mathop{\mathrm{T}}_{RxE}), \tag{4}$$

where  $\mathop{\mathrm{E}}{\mathrm{T}}_E$  and  $\mathop{\mathrm{B}}{\mathrm{T}}_{B'}$  refer to the safe distances for grippers approaching *Member 2* and moving away from *Member 1* linearly.  $\mathop{\mathrm{R}}_{RxE} \mathop{\mathrm{T}}_{RxE}$  is the operation in order to use the same inverse kinematics as in the case of  $\mathop{\mathrm{B}}{\mathrm{T}}_E$ , while the robot interchanges grippers for attaching.  $\mathop{\mathrm{T}}_{RxE}$  is the matrix indicating a pure rotation around the  $x$ -axis by  $\pi$ , as

$$\mathop{\mathrm{T}}_{RxE} = \begin{bmatrix} \mathbf{R}_x(\pi) & \mathbf{0} \\ \mathbf{0} & 1 \end{bmatrix} = \begin{bmatrix} 1 & 0 & 0 & 0 \\ 0 & -1 & 0 & 0 \\ 0 & 0 & -1 & 0 \\ 0 & 0 & 0 & 1 \end{bmatrix}. \tag{5}$$

Equation (2) reflects the constraints on reachability, while Equations (3) and (4) reflect accessibility.

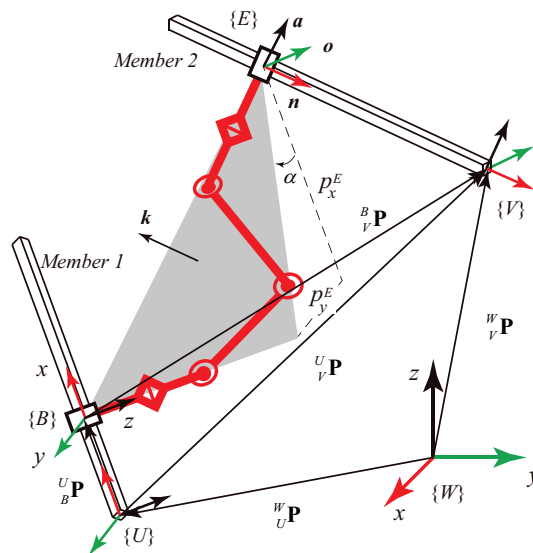


Figure 5. The diagram for transition analysis.

### 3. Transition Analysis

Transition analysis will be the core component called frequently by the global path planner. In order to rapidly determine whether a member-to-member transition is feasible, hierarchical inspections are conducted in transition analysis. Preliminary requirements for reachability and safety are firstly applied to distinguish apparently infeasible transitions. Strict constraints are then considered to compute the operational region for transition. In this section, we first present the preliminary requirements, and then move on to the strict constraints. The implementation of corresponding algorithms will be presented in Section 4.

#### 3.1. Preliminary Requirements

A transition is definitely infeasible if the target gripping position is out of reach by a BiCR. Denoting  $D$  as the distance between two members, the first preliminary requirement is,

$$D \leq \sum_{i=0}^n l_i, \tag{6}$$

where  $n$  stands for the degrees of freedom of the robot, and  $l_i$  for the lengths of the robot linkages.

Normally, dynamics and gripping force should be analyzed and controlled to ensure the safety of each grip. However, in the global path planning stage, the robot’s trajectory is not yet determined and is thereby unknown, regardless of strict verification of grip safety. Observing the geometrical constraints between grippers and members, we use prior knowledge from statics for preliminary safety checks in this paper.

Some BiCRs, for instance, 3DCLIMBER and Climbot mentioned in Section 1, are designed with grippers configuring perpendicular V-shaped grooves as palms. When enclosing members of square or circular cross sections, resulting grips can be classified into four categories according to the circumferential torque required and difficulties for balance, as shown in Figure 6. Suppose the biggest gripping force is always acting on thereby the gripper will never open. Among the above grips, gripping an upright cylindrical or a square member is always safe, no matter how the robot moves, as illustrated in Figure 6a,b. However, when gripping a slanted cylindrical member from an upright direction, as indicated in Figure 6c, the robot has no guarantee of safety, which depends on its motion. More exactly, the robot movement will be limited in an upright plane, in which case there is no circumferential torque generated by gravity. Finally, gripping slanted cylindrical members in other orientations, as illustrated in Figure 6d, is unsafe because the gripper cannot generate sufficient friction force to resist the huge circumferential torque caused by gravity. Taking the Climbot for example to estimate, the gripper must be able to generate a clamping force of 27,000 N to resist the gravity in the worst case. Denoting  $R$  as the spatial relationship between *Member 1* and *Member 2*, and  $\mathbf{d}_G \in \mathbb{R}^3$  as the unit direction vector of the gravity, another preliminary requirement can be expressed as,

$$\neg\{[(\|\mathbf{d}_1 \times \mathbf{d}_G\| = 0 \wedge \zeta_1 = 0) \vee (\|\mathbf{d}_2 \times \mathbf{d}_G\| = 0 \wedge \zeta_2 = 0)] \wedge R = \textit{staggered or parallel}\}, \quad (7)$$

where  $\zeta_1$  and  $\zeta_2$  are flags indicating the cross section type of members. For example,  $\zeta_1 = 0$  if the cross section of *Member 1* is cylindrical. Otherwise  $\zeta_1 = 1$ . In addition, movement constraints could be recorded for future usage in the cases of  $R = \textit{intersecting or collinear}$ .

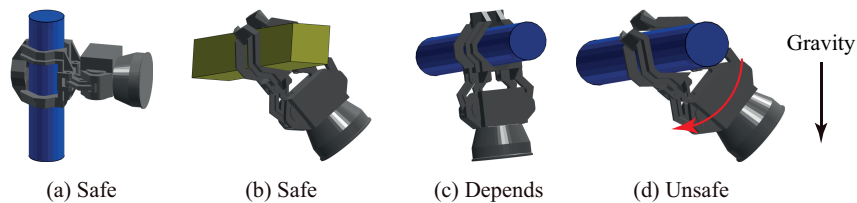


Figure 6. Four categories of grips.

### 3.2. Strict Constraints

To reach an arbitrary configuration in 3D space, a manipulator needs at least 6 DoF. Hence, a 6DoF BiCR is capable of transiting between any two members with any target orientation. However, with respect to 5DoF BiCRs, such as Climbot, the reachability of its end effector, particularly in terms of orientation, is obviously limited. It has been verified in [31] that 5 DoF in planar configuration is a reasonable trade-off between dexterity and physical limitations such as power of actuators. Accordingly, transitions with 5DoF BiCRs and given members should be analyzed strictly.

From the transition model stated in Section 2.2, for each pair of gripping points, one on *Member 1* and another on *Member 2*, the reachability is equivalent to the existence of solutions when solving the robot inverse kinematics. Motivated by this observation, we first describe *Member 2* with respect to the coordinate frame  $\{B\}$ . From Figure 5, we can directly write down

$${}^B_V P = {}^U_V P - {}^U_B P, \quad (8)$$

where  ${}^U_B\mathbf{P} = [t_1 \ 0 \ 0]^T$ . Then, expressing the origin of  $\{V\}$  with respect to  $\{U\}$  yields,

$$\begin{bmatrix} {}^U_V\mathbf{P} \\ 1 \end{bmatrix} = {}^U_W\mathbf{T} \begin{bmatrix} {}^W_V\mathbf{P} \\ 1 \end{bmatrix} = \begin{bmatrix} {}^W_U\mathbf{R}^T & -{}^W_U\mathbf{R}^T {}^W_U\mathbf{P} \\ \mathbf{0} & 1 \end{bmatrix} \begin{bmatrix} {}^W_V\mathbf{P} \\ 1 \end{bmatrix} = \begin{bmatrix} {}^W_U\mathbf{R}^T ({}^W_V\mathbf{P} - {}^W_U\mathbf{P}) \\ 1 \end{bmatrix}. \tag{9}$$

Substituting Equation (9) into Equation (8), we obtain the reference origin of *Member 2* with respect to  $\{B\}$  as,

$${}^B_V\mathbf{P} = {}^W_U\mathbf{R}^T ({}^W_V\mathbf{P} - {}^W_U\mathbf{P}) - {}^U_B\mathbf{P}. \tag{10}$$

The direction unit vector of *Member 2* can be easily transformed to  $\{B\}$  as  ${}^B\mathbf{d}_2 = {}^U_B\mathbf{R}^{-1} {}^W_U\mathbf{R}^{-1} {}^W\mathbf{d}_2$ . Thus, we have

$${}^B_E\mathbf{P} = {}^B_V\mathbf{P} + t_2 {}^B\mathbf{d}_2. \tag{11}$$

### 3.2.1. Orientation Constraints

Considering orientation constraints, we propose and prove two propositions which are important for analyzing the member-to-member transition problem with BiCRs, such as Climbot. Note that variable symbols without superscript are used with respect to frame  $\{B\}$  hereafter.

**Proposition 1.** *Given the current base at  $\{B\}$  and the goal gripping orientation  ${}^B_E\mathbf{R} = [\mathbf{n} \ \mathbf{o} \ \mathbf{a}]$ , there exists only one feasible configuration for BiCRs, such as Climbot, to transit between two staggered members.*

**Proof.** Due to the structural configuration of Climbot, its links are always in a plane (“robot plane” for short, highlighted in gray in Figure 5). Therefore, the following orientation constraints must be satisfied,

$$\begin{cases} \mathbf{k} \cdot \mathbf{a} = 0 \\ \tan \alpha = p_y^E / p_x^E \end{cases} \tag{12}$$

where  $\mathbf{k} = [-\sin \alpha \ \cos \alpha \ 0]^T$  represents the norm vector of the robot plane. Substituting Equation (11) and  $\mathbf{n} = \mathbf{d}_2$  into Equation (12) yields

$$t_2 = \frac{p_x^V a_y - p_y^V a_x}{n_y a_x - n_x a_y}. \tag{13}$$

On the right side of Equation (13), the values are all constants. Hence, we obtain a unique gripping position for feasible transition by substituting  $t_2$  into Equation (11), when  $n_y a_x - n_x a_y \neq 0$ . □

It should be underlined that *Member 2* is on the robot plane when  $n_y a_x - n_x a_y = 0$ . Therefore, all points on *Member 2* satisfy the orientation constraints. In this case, a gripping point on *Member 1* may correspond to unlimited gripping points on *Member 2* for feasible transition. The graspable region determination algorithm presented in [31] could be applied to this case by sampling attaching positions on both members in order to quickly obtain some operational regions for transition.

**Proposition 2.** *For BiCRs, such as Climbot, to transit between two staggered members, given the base and the goal gripping orientations as  ${}^W_U\mathbf{R}$  and  ${}^W_V\mathbf{R}$ , respectively, the operational region for transition on *Member 2* is linear with that on *Member 1*.*

**Proof.** Recall Equation (10), and set  $\lambda = {}^W_U\mathbf{R}^T ({}^W_V\mathbf{P} - {}^W_U\mathbf{P})$ .  ${}^B_V\mathbf{P}$  can be written as

$${}^B_V\mathbf{P} = [p_x^V \ p_y^V \ p_z^V]^T = \begin{bmatrix} -t_1 + \lambda_x \\ \lambda_y \\ \lambda_z \end{bmatrix}. \tag{14}$$



Note that since  ${}^W_U\mathbf{R}$ ,  ${}^W_V\mathbf{P}$ , and  ${}^W_U\mathbf{P}$  are all known invariants,  $\lambda$  is actually a constant vector. Substituting Equation (14) into Equation (13) results in

$$t_2 = \frac{(-t_1 + \lambda_x)a_y - \lambda_y a_x}{n_y a_x - n_x a_y} = \sigma t_1 + \delta, \tag{15}$$

where  $\sigma = -a_y / (n_y a_x - n_x a_y)$ , and  $\delta = (\lambda_x a_y - \lambda_y a_x) / (n_y a_x - n_x a_y)$ . Both  $\sigma$  and  $\delta$  are constants. Therefore,  $t_2$  and  $t_1$  are linear, and thereby have one-to-one mapping with each other. Once  $t_1$  is determined,  $t_2$  can be calculated by Equation (15), and vice versa.  $\square$

### 3.2.2. Position Constraints

To confirm whether the transition is feasible, we need to further investigate if  ${}^B_E\mathbf{P}$  is within the reachable workspace of the robot. Reflected in solving the inverse kinematics, the following inequality must be satisfied,

$$c_3 = \left| \frac{(p'_x c_1 + p'_y s_1)^2 + (p'_z - l_{01})^2 - (l_2^2 + l_3^2)}{2l_2 l_3} \right| \leq 1, \tag{16}$$

where  $c_1 \triangleq \cos \theta_1$ ,  $s_1 \triangleq \sin \theta_1$ , and  $l_{01} \triangleq l_0 + l_1$  (similar expressions are used for shorthand hereafter);  $\tan \theta_1 = a_y / a_x$ , and  $\mathbf{P}' = \mathbf{P}^V + t_2 \mathbf{n} - l_{45} \mathbf{a}$  represents the position vector of the wrist joint of the robot, e.g.,  $T_2$  in Figure 2 for Climbot. Let  $\omega_1 = p'_x c_1 + p'_y s_1$ , and  $\omega_2 = p'_z - l_{01}$ , and denote  $\theta_{lim}$  as the rotation limitation of joint  $T_0$  (see Figure 2). Since  $l_2 = l_3$  for Climbot, Equation (16) can be simplified as

$$2l_2 \cos \frac{\theta_{lim}}{2} \leq \omega_1^2 + \omega_2^2 \leq 4l_2^2. \tag{17}$$

Utilizing  $t_1$  (Equation (15)) to express  $\omega_1^2 + \omega_2^2$ , we have

$$\omega_1^2 + \omega_2^2 = (A^2 + C^2)t_1^2 + 2(AB + CD)t_1 + B^2 + D^2, \tag{18}$$

where  $A = \sigma(n_x c_1 + n_y s_1) - c_1$ ,  $B = (\delta n_x - a_x l_{45} + \lambda_x)c_1 + (\delta n_y - a_y l_{45} + \lambda_y)s_1$ ,  $C = \sigma n_z$ ,  $D = \delta n_z - a_z l_{45} + \lambda_z - l_{01}$ .

Let  $f(t_1) = \omega_1^2 + \omega_2^2 - 4l_2^2$ , and  $g(t_1) = \omega_1^2 + \omega_2^2 - 2l_2 \cos \frac{\theta_{lim}}{2}$ . Equation (17) can be converted to two quadratic functions, as

$$f(t_1) = Et_1^2 + Ft_1 + G \leq 0, \tag{19}$$

$$g(t_1) = Et_1^2 + Ft_1 + H \geq 0, \tag{20}$$

where  $E = (A^2 + C^2)$ ,  $F = 2(AB + CD)$ ,  $G = B^2 + D^2 - 4l_2^2$ , and  $H = B^2 + D^2 - 2l_2 \cos \frac{\theta_{lim}}{2}$ .

In fact, Equation (19) accounts the reachability of the robot, while Equation (20) is the constraint from the rotation limitation of joint  $T_0$ . Therefore, discriminants of  $f(t_1)$  and  $g(t_1)$  determine the feasibility and distribution of operational regions for transition, with the correspondences listed in Table 1.

**Table 1.** Discriminants corresponding to the distribution of operational regions for transition.

| Discriminants <sup>a</sup>      | Distribution <sup>b</sup>  | Operational Regions       |
|---------------------------------|--|---------------------------|
| $\Delta_1 < 0$                  | Out of the workspace   | No                        |
| $\Delta_1 = 0, \Delta_2 > 0$    | Out of the rotation limitation   | No                        |
| $\Delta_1 = 0, \Delta_2 \leq 0$ | On the boundary of the workspace   | Unique point              |
| $\Delta_1 > 0, \Delta_2 \leq 0$ | Within the workspace and rotation limitation                             | One segment               |
| $\Delta_1 > 0, \Delta_2 > 0$    | Within the workspace but some points beyond rotation limitation of $T_0$ | Two segments <sup>c</sup> |

<sup>a</sup>  $\Delta_1 = F^2 - 4EG$  and  $\Delta_2 = F^2 - 4EH$  are discriminants of Equations (19) and (20), respectively. <sup>b</sup> The gripping points on Member 1 satisfying the orientation constraints are described. <sup>c</sup> The two segments have equal lengths and are symmetric about  $-F/(2E)$ .

Solving Equations (19) and (20), the operational regions on *Member 1* and *Member 2*, respectively, satisfying Equation (2) could be obtained. Similar processes should be conducted for Equations (3) and (4), to discard those reachable but not accessible gripping points from the obtained operational regions.

### 3.2.3. Length Constraints

Since a real member has limited length, we need to verify whether the obtained operational regions are on the given members or not. In other words,  $t_1$  and  $t_2$  have to satisfy

$$\begin{cases} 0 \leq t_1 \leq L_1 \\ 0 \leq t_2 \leq L_2 \end{cases} \quad (21)$$

where  $L_1$  and  $L_2$  stand for the lengths of the two members, respectively.

An effective way to constrain the operational regions on members is by mapping the length limitation of *Member 2* to  $t_1$  using Equation (15),

$$\begin{cases} \underline{t}'_1 = \min \left( -\frac{\delta}{\sigma'}, \frac{L_2 - \delta}{\sigma} \right) \\ \bar{t}'_1 = \max \left( -\frac{\delta}{\sigma'}, \frac{L_2 - \delta}{\sigma} \right) \end{cases} \quad (22)$$

Supposing the operational regions on *Member 1* from Section 3.2.2 are  $[\underline{t}_1, \bar{t}_1]$ , the real operational regions for the base gripper satisfying constraints including the reachability, accessibility, rotation limitation of  $T_0$ , and length limitations become

$$t_1 = [0, L_1] \cap [\underline{t}_1, \bar{t}_1] \cap [\underline{t}'_1, \bar{t}'_1]. \quad (23)$$

The corresponding operational regions for the swinging gripper on *Member 2* can be updated by Equation (15).

### 3.2.4. Other Constraints

Besides the above constraints, if the rotation limitations of joints  $T_1$  and  $T_2$  are also taken into account, we additionally need to check whether their rotation is in a valid range. This could be done through solving the inverse kinematics when gripping endpoints of  $t_1$  from Equation (23). Those parts of  $t_1$  and  $t_2$  corresponding to invalid movements should be discarded. An effective method to accomplish this test can be found in [31].

Finally, we obtain accurate and complete operational regions. Holding points involved in these regions, the robot is able to perform the transition from a member to another. Naturally, if the operational region is empty, there is no feasible transition. Note that the presented transition analysis is mainly based on the existence of solutions to a set of quadratic functions. Therefore, it is capable of obtaining the complete solution if the operational region exists for BiCRs, such as Climbot, or with fewer degrees of freedom.

## 4. Fast Determination of Feasible Global Paths

Making use of the proposed transition analysis, we present a novel effective and efficient path planning approach in this section to address the global route fast determination problem for BiCRs moving on spatial trusses.

### 4.1. Principle and Flowchart

The basic idea is to find out all the feasible routes from the current state based on our transition analysis in Section 3, and then reserve only those terminated at the expected destination. Tree data

structure is a good choice to organize the route exploration and record all the feasible routes. Each node of a tree stores the information of a member and associated operational regions for transiting to from its parent node (the former member). Let the member the robot initially grips on be the root node and ensure the leaf nodes represent the destination member. In this way, each route from the root to the leaf forms a global path from the original point to the destination, containing the necessary information for transition, i.e., members and operational regions. Figure 7 shows us the flowchart.

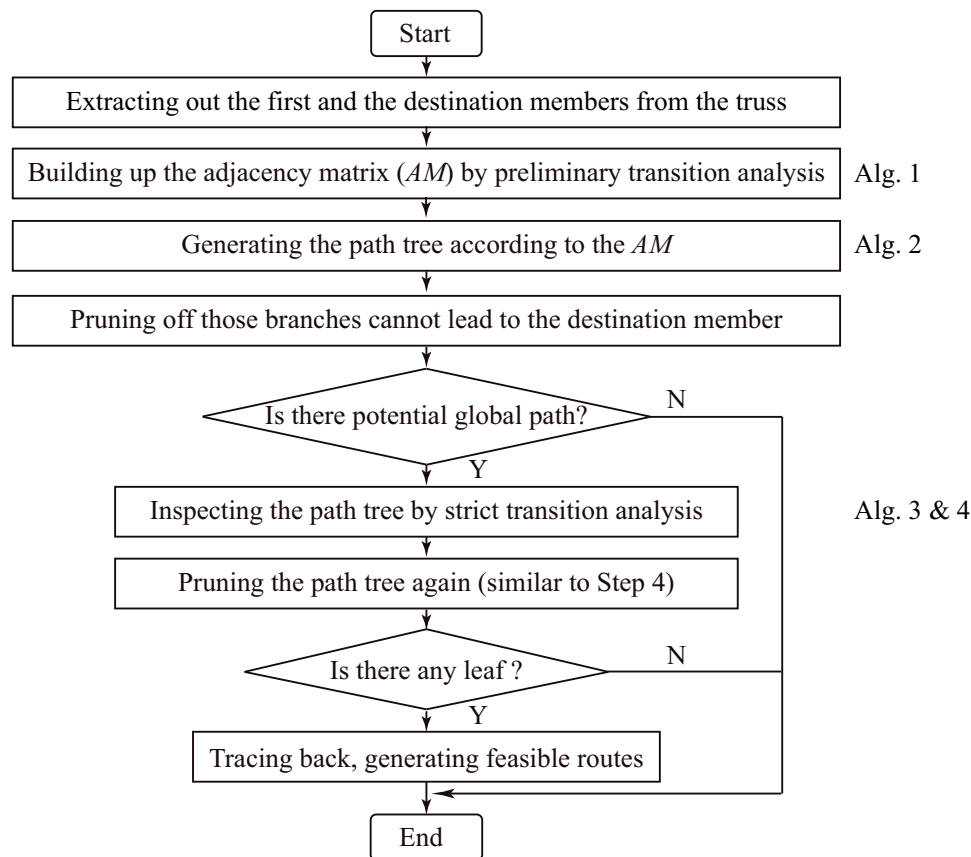


Figure 7. The flowchart of global path planning.

First of all, the original and destination members are extracted by checking which members the points  ${}^W_B P_{init}$  and  ${}^W_B P_{goal}$  are located on.

Secondly, all the members are checked in pairs with preliminary requirements in Equations (6) and (7). The results are stored in an adjacency matrix, as shown in Algorithm 1. Elements of this matrix refer to the preliminary possibility of transition between two members indicated by the row and the column indexes.

Thirdly, a tree data structure (path tree for short) rooted at the original member is then built up according to the adjacency matrix and the following rules, as in Algorithm 2.

- Never go backwards.
- Stop going forwards only when either the destination member is reached or there is no member that it has never been to.

Those branches not terminated at the destination member are pruned off promptly in order to keep the tree data structure on a small scale, which is helpful for improving the solving efficiency.

Fourthly, the above path tree will be traversed and inspected by analyzing strict constraints for transition presented in Section 3.2 and shown in Algorithm 3. This process starts from the root and spreads to the leaves. In other words, each route from the root to any of leaves will be inspected.

Branches will be grafted onto the tree if more than one possible gripping orientations result in operational regions for transition. Conversely, a branch will be pruned off once its corresponding transition is verified to be impossible. It should be noted that the pruning operation must ensure that the tree leaves can only be the destination member at this moment. After traversing the entire tree, the remaining routes if any, are feasible global paths.

Finally, feasible global paths are obtained by tracing back from the leaves to the root. Each route consists of a sequence of members with specific gripping orientations and the corresponding operational regions for transition.

---

**Algorithm 1:** Building up the adjacency matrix
 

---

**Input:**  $^W S$ : the truss;  
 $l_i$ : lengths of robot linkages.  
**Output:**  $AM$ : the adjacency matrix.

- 1:  $N \leftarrow \text{NUMBEROFMEMBERS}(^W S)$
- 2: **for**  $i = 1$  **to**  $N - 1$  **do**
- 3:   **for**  $j = i + 1$  **to**  $N$  **do**
- 4:      $M_i \leftarrow \text{GETMEMBER}(^W S, i)$ ;
- 5:      $M_j \leftarrow \text{GETMEMBER}(^W S, j)$
- 6:      $D \leftarrow \text{DISTANCE}(M_i, M_j)$ ;
- 7:      $R \leftarrow \text{RELATIONSHIP}(M_i, M_j, ^W G)$ ;
- 8:     **if**  $D$  and  $R$  satisfy Equations (6) and (7) **then** // Transition may be possible
- 9:        $AM(i, j) \leftarrow \text{true}$ ,  $AM(j, i) \leftarrow \text{true}$ ;
- 10:    **else** // Transition is definitely impossible
- 11:       $AM(i, j) \leftarrow \text{false}$ ,  $AM(j, i) \leftarrow \text{false}$ ;
- 12:    **end if**
- 13:   **end for**
- 14:    $AM(i, i) \leftarrow \text{false}$ ;
- 15: **end for**

---



---

**Algorithm 2:** Generating the path tree
 

---

**Input:**  $AM$ : the adjacency matrix;  
 $\chi(i)$ : the member the robot moving on in current iteration;  
 $\chi(m)$ : the destination member;  
 $T$ : the path tree from last iteration.  
**Output:**  $T$ : the path tree updated in each iteration.

- 1:  $M^{\text{potential}} \leftarrow \text{GETPOTENTIALMEMBERS}(AM, \chi(i))$ ;
- 2:  $M^{\text{passed}} \leftarrow \text{GETPASTMEMBERS}(T, \chi(i))$ ;
- 3: **for**  $j = 1$  **to**  $\text{NUMBEROFMEMBERS}(M^{\text{potential}})$  **do**
- 4:   **if**  $M_j^{\text{potential}} = \chi(m)$  **then** // Reach the destination member
- 5:     **return**  $T.\text{ADDNODE}(T, \chi(m))$ ;
- 6:   **else** // Continue to explore
- 7:     **if**  $M_j^{\text{potential}} \notin M^{\text{passed}}$  **then** // New potential member never visited
- 8:        $T.\text{ADDNODE}(T, M_j^{\text{potential}})$ ;
- 9:       call Algorithm 2( $AM, M_j^{\text{potential}}, \chi(m), T$ ); // Recursively call the algorithm itself
- 10:     **end if**
- 11:   **end if**
- 12: **end for**

---

**Algorithm 3:** Inspecting the path tree

---

**Input:**  $^W S$ : the truss;  
 $^W_B R_{init}$ : initial gripping orientation for base gripper;  
 $^W_B R_{goal}$ : final gripping orientation for base gripper;  
 $T$ : the pruned path tree from Algorithm 2.

**Output:**  $T^{ori}$ : path tree with operational regions and corresponding gripping orientations.

```

1:  $iter \leftarrow T.BREADTHFIRSTITERATOR()$ ; // Generate iterators to traverse nodes
2:  $T^{ori}.INITIALIZE(^W_B R_{init}, T.GETROOT())$ ;
3:  $i \leftarrow 2$ ;
4: while  $i < NUMBER(iter)$  do
5:    $N^{Parent} \leftarrow T.GETPARENTNODE(iter(i))$ ;
6:    $M1 \leftarrow GETMEMBER(^W S, N^{Parent})$ ;
7:    $M2 \leftarrow GETMEMBER(^W S, T.GETNODE(iter(i)))$ ;
8:   for  $j = 1$  to  $T.NUMBEROFPARENTS(iter(i))$  do
9:      $^W_U R \leftarrow T.GETGRIPORIENT(iter(i), j)$ ; // Extract corresponding gripping orientation
10:    if  $T.ISLEAF(iter(i))$  then // Reach the destination member
11:       $^W_V R \leftarrow ^W_B R_{goal}, K = [1]$ ;
12:    else if  $\zeta_{M2} = 0$  then // Transition to a cylindrical member
13:       $^W_V R \leftarrow SELECTORIENTATION(M2), K = [1]$ ;
14:    else // Transition to a squared member
15:       $^W_V R \leftarrow T.INITGRIPORIENTATION(M2)$ ;
16:       $K = [1, 2, 3, 4]$ ;
17:    end if
18:    for each  $k$  in  $K$  do // Check each potential gripping orientation
19:       $(t_1, t_2) \leftarrow \text{Algorithm 4}(M1, M2, ^W_U R, ^W_V R)$ ;
20:      if  $t_1 \neq \emptyset$  then // Transition is feasible
21:         $T^{ori}.ADDNODE(iter(i), ^W_V R, t_1, t_2)$ ;
22:      end if
23:       $^W_V R \leftarrow R_n(\pi/2)^W_V R$ ; // Prepare for another gripping orientation
24:    end for
25:  end for
26:   $i++$ ;
27: end while

```

---

#### 4.2. Algorithms

Algorithm 1 shows us the implementation of building up the  $N \times N$  symmetric adjacency matrix. Each element of the matrix stores a binary value, indicating whether a pair of members is transitable or not, i.e., the transition between *Member i* and *Member j* is possible if  $AM(i, j) = true$  and impossible if  $AM(i, j) = false$ . The probabilities for transition between each pair of members are inspected successively, according to the preliminary requirements concerning about the reachability and safety, i.e., Equations (6) and (7). Binary values are then assigned to corresponding elements.

Algorithm 2 implements the generation of the path tree according to the adjacency matrix from Algorithm 1, and the original and destination members. Algorithm 2 is actually a recursive function that calls itself iteratively, so that the path tree “grows up” from the root to leaves step by step. During each iteration, it extracts all transitable members from the current one, removes those visited, then adds the remaining members to the path tree. Such an iteration repeatedly goes on until the robot arrives at the destination member or has no new members to visit. The obtained path tree should be “scanned” and pruned if necessary, keeping only those branches with the destination member as leaves.

Algorithm 3 traverses the obtained path tree in a breadth-first sequence, inspecting all transitions from a parent node to the present one with strict constraints. For squared members, all four gripping directions will be sent to Algorithm 4 for inspection. This is because a squared member has four potential gripping directions for a V-shaped palm gripper, which are around its center axis by an angular interval of  $\pi/2$ . As a result, new branches may be grafted onto the path tree if more than one gripping directions result in operational regions for transition. Regarding the transit to an upright cylindrical member, the possible gripping directions are unlimited, as demonstrated in Equation (13). In this case, we can select an optimal gripping direction, for example to balance the difficulties of two consecutive transitions, i.e., from the parent node to the present one, and from the present node to the child one.

---

**Algorithm 4:** Solving operational regions for transition
 

---

**Input:**  ${}^W_U P$ : reference point of *Member 1*;  
 ${}^W_V P$ : reference point of *Member 2*;  
 ${}^W_U R$ : gripping orientation on *Member 1*;  
 ${}^W_V R$ : gripping orientation on *Member 2*.  
**Output:**  $t_1$ : operational region for transition on *Member 1*;  
 $t_2$ : operational region for transition *Member 2*;  
 1: calculate intermediate variables:  $\sigma, \delta, A \sim H$ ;  
 2:  $\Delta_1 \leftarrow F^2 - 4EG, \Delta_2 \leftarrow F^2 - 4EH$ ;  
 3: **if**  $\Delta_1 < 0$  or ( $\Delta_1 = 0$  and  $\Delta_2 > 0$ ) **then** // No operational region for transition  
 4:   **return**  $t_1 \leftarrow \emptyset, t_2 \leftarrow \emptyset$ ;  
 5: **else if**  $\Delta_1 = 0$  **then** // Unique configuration  
 6:    $t_1 \leftarrow -F/(2E)$ ;  
 7: **else if**  $\Delta_1 > 0$  and  $\Delta_2 \leq 0$  **then** // A segment of operational region  
 8:    $t_1 \leftarrow \left[ \frac{-F-\sqrt{\Delta_1}}{2E}, \frac{-F+\sqrt{\Delta_1}}{2E} \right]$ ;  
 9: **else if**  $\Delta_1 > 0$  and  $\Delta_2 > 0$  **then** // Two segments of operational regions  
 10:    $t_1 \leftarrow \left[ \frac{-F-\sqrt{\Delta_1}}{2E}, \frac{-F-\sqrt{\Delta_2}}{2E} \right] \cup \left[ \frac{-F+\sqrt{\Delta_2}}{2E}, \frac{-F+\sqrt{\Delta_1}}{2E} \right]$ ;  
 11: **end if**  
 12: check accessibility according to Equations (3) and (4); // Similar to Line 1 to 11  
 13: restrict  $t_1$  according to Equation (23);  
 14: check rotation limitations of other joints and modify  $t_1$ ;  
 15: **if**  $t_1 \neq \emptyset$  **then** // Transition feasible  
 16:    $t_2 \leftarrow \sigma t_1 + \delta$ ;  
 17: **else** // Transition infeasible  
 18:    $t_2 \leftarrow \emptyset$ ;  
 19: **end if**

---

Algorithm 4 details the procedure to compute operational regions for each to-be-inspected transition, dispatched from Algorithm 3. The reachability is firstly taken into account to generate one or two segments of regions on *Member 1* for further inspection, according to Table 1. After that, the resulting operational regions will be shortened if (a) points are not accessible; (b) points are not on *Member 2*; or (c) corresponding movement is beyond the robot joints' rotation limitation. Operational regions on *Member 2* will be finally computed according to Equation (15).

## 5. Simulations

To verify the proposed analysis and algorithms, simulations are conducted with Climbot. A simulation environment is developed and algorithms are implemented on the platform of MATLAB R2015b. All the simulations are launched on a desktop with Intel Core i7-7700K CPU and 16 GB RAM, running with the 64-bit operating system Windows 10 Pro.

5.1. Result of Transition Analysis

The first part of the simulations is to verify the effectiveness of transition analysis. In this simulation, given two arbitrary squared members in spatial environments, the aim is to solve the operational regions for transition. The two members used for illustration in this paper are

$${}^wS = \begin{Bmatrix} 1187 & 372 & 692 & 428 & 150 & 878 & 1 & 0.5 \\ 225 & 1182 & 1331 & 550 & 807 & 603 & 1 & 9 \end{Bmatrix} \quad (24)$$

where each row represents a member, with the parameters  $P_1 \in \mathbb{R}^3$ , and  $P_2 \in \mathbb{R}^3$  successively standing for positions of end points, and  $\zeta \in \mathbb{R}^1$  and  $\psi \in \mathbb{R}^1$  indicating the cross-section type and the rotating angle around the member's own axis, respectively.

Figure 8 shows the simulation result of transition analysis. Without consideration of the accessibility of grips, there are four possible cases for transiting from *Member 1* to *Member 2*, with different gripping orientations on the two members, respectively, as shown in Figure 8a. The operational regions are highlighted in green to distinguish them from the other parts of the member. Robots are displayed in specific configurations corresponding to the boundaries of operational regions. Taking the accessibility of grips into account, there remain only two possible cases for transition, as shown in Figure 8b. Moreover, the obtained operational regions in these two possible cases are narrowed down. Shortened parts, painted in red in Figure 8b, must be discarded, owing to corresponding grips being reachable but not accessible.

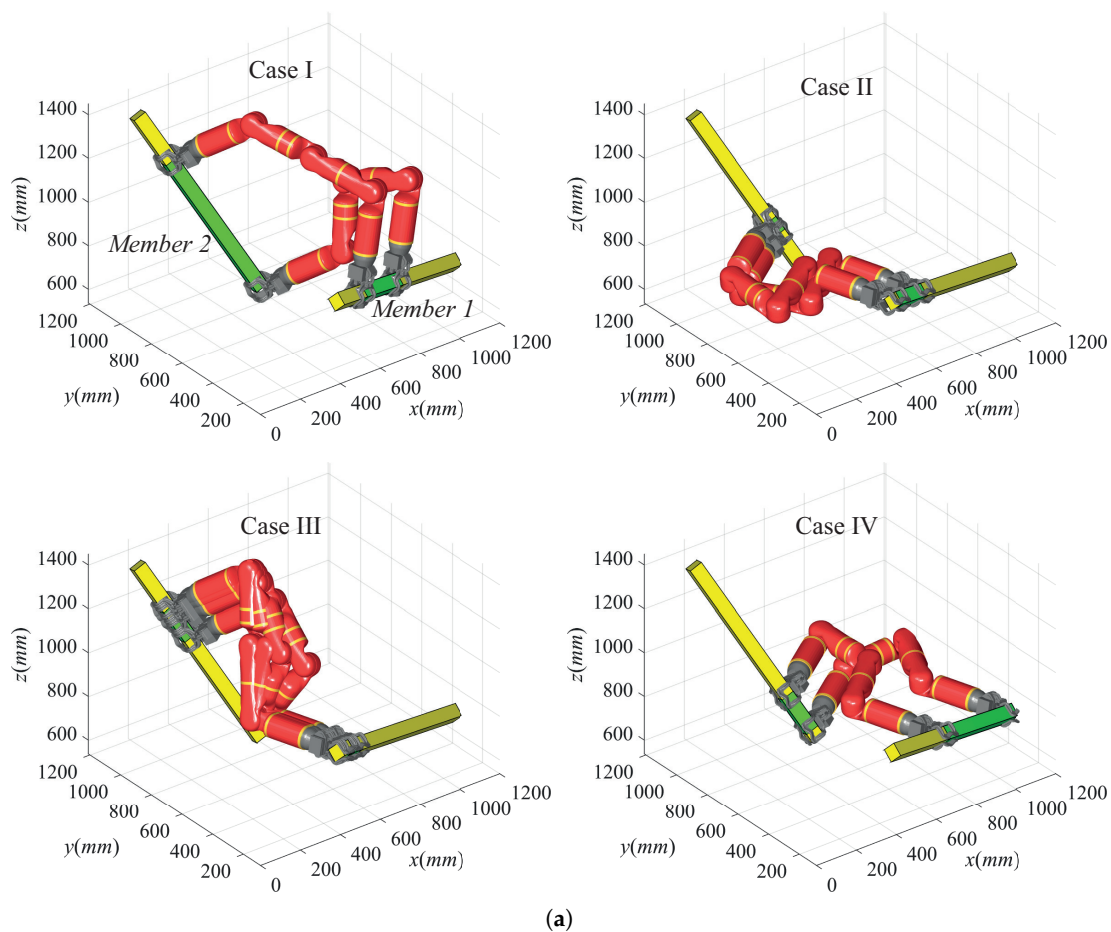
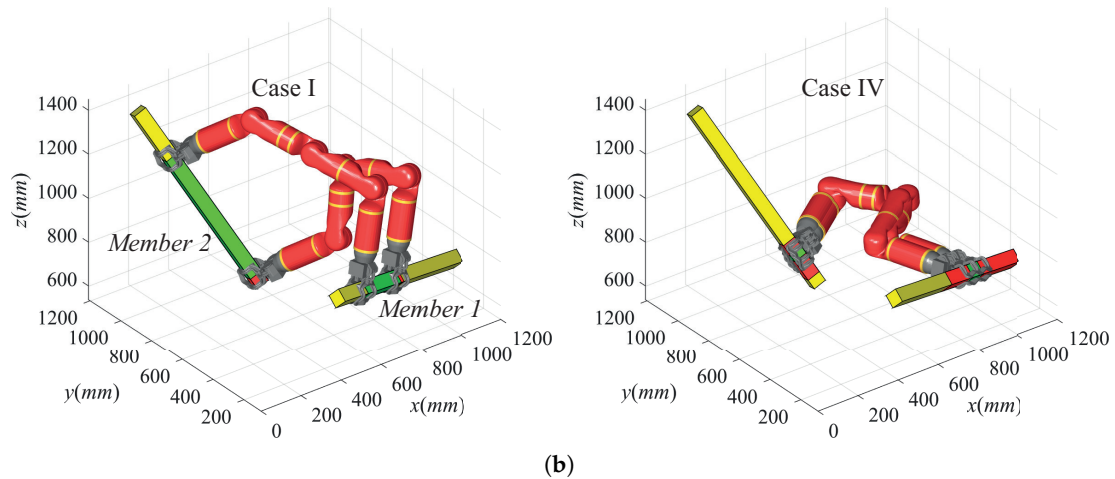


Figure 8. Cont.



**Figure 8.** Results of member-to-member transition analysis: (a) without the consideration of grip accessibility; (b) considering grip accessibility (no operational region for the cases II and III shown in Sub-figure (a)).

Table 2 quantitatively compares the operational regions for transition, computed with and without a consideration of the robot’s accessibility. From the table, if the accessibility is taken into account, all the operational regions in four cases are shortened, with a percentage from 7.3% to 100%. To further investigate the importance of considering accessibility, we conducted 1000 rounds of comparative transition analysis with randomly-generated members. In total 94.6% of operational regions were narrowed down, with an average shortening percentage of 59.9% at a time cost of 32.7 ms (over 19.6 ms if we do not account for accessibility). In fact, configurations corresponding to the boundaries always suffer from singularity or joint rotation limitation. When planning specific grips subsequently, optimal grips should keep a distance from the boundaries of operational regions. Therefore, it is necessary to consider accessibility in addition to reachability for each grip.

**Table 2.** Comparison of transition analysis results with and without the consideration of accessibility.

| Characteristics | Operational Regions <sup>a</sup> |                                 | Shortening Percentage <sup>b</sup> |
|-----------------|----------------------------------|---------------------------------|------------------------------------|
|                 | On Member 1                      | On Member 2                     |                                    |
|                 |                                  | Case I                          |                                    |
| Without         | [408, 653.7]                     | [881.0, 229.35]                 | 7.3%                               |
| With            | [426.7, 653.7]                   | [831.4, 229.3]                  |                                    |
|                 |                                  | Case II                         |                                    |
| Without         | [628.6, 801.0]                   | [600.0, 535.0]                  | 100.0%                             |
| With            | \                                | \                               |                                    |
|                 |                                  | Case III                        |                                    |
| Without         | [694.0, 742.6] ∪ [760.9, 770.1]  | [760.9, 770.1] ∪ [230.5, 212.2] | 100.0%                             |
| With            | \                                | \                               |                                    |
|                 |                                  | Case IV                         |                                    |
| Without         | [0, 470.6]                       | [837.0, 660.0]                  | 84.5%                              |
| With            | [252.0, 325.0]                   | [742.0, 714.5]                  |                                    |

<sup>a</sup> Represented with parameters of  $t_1$  and  $t_2$ , respectively. <sup>b</sup> Computed as  $1 - \Delta t'_1 / \Delta t_1$ , where  $\Delta t'_1$  and  $\Delta t_1$  refer to operational regions with and without the consideration of accessibility.

### 5.2. Result of Global Path Determination

The second part of the simulation is to verify the proposed algorithms used to determine global paths. Two virtual truss scenes, simple and complicated, consisting of 7 and 25 members, respectively, were deployed for validation. Figures 9 and 10 show us the results. In the simulation, the starting



point and the destination are specified manually but arbitrarily, highlighted with a green and a red sphere, respectively. The feasible global routes are illustrated with member-to-member transitions. Corresponding operational regions for transition are also highlighted with green. Nearby numbers indicate the sequence of transitions to be performed along the way. Sub-figures on the right side are simplified diagrams of routes for easy understanding. Arrows indicate the directions Climbot goes forwards from the starting point to the destination.

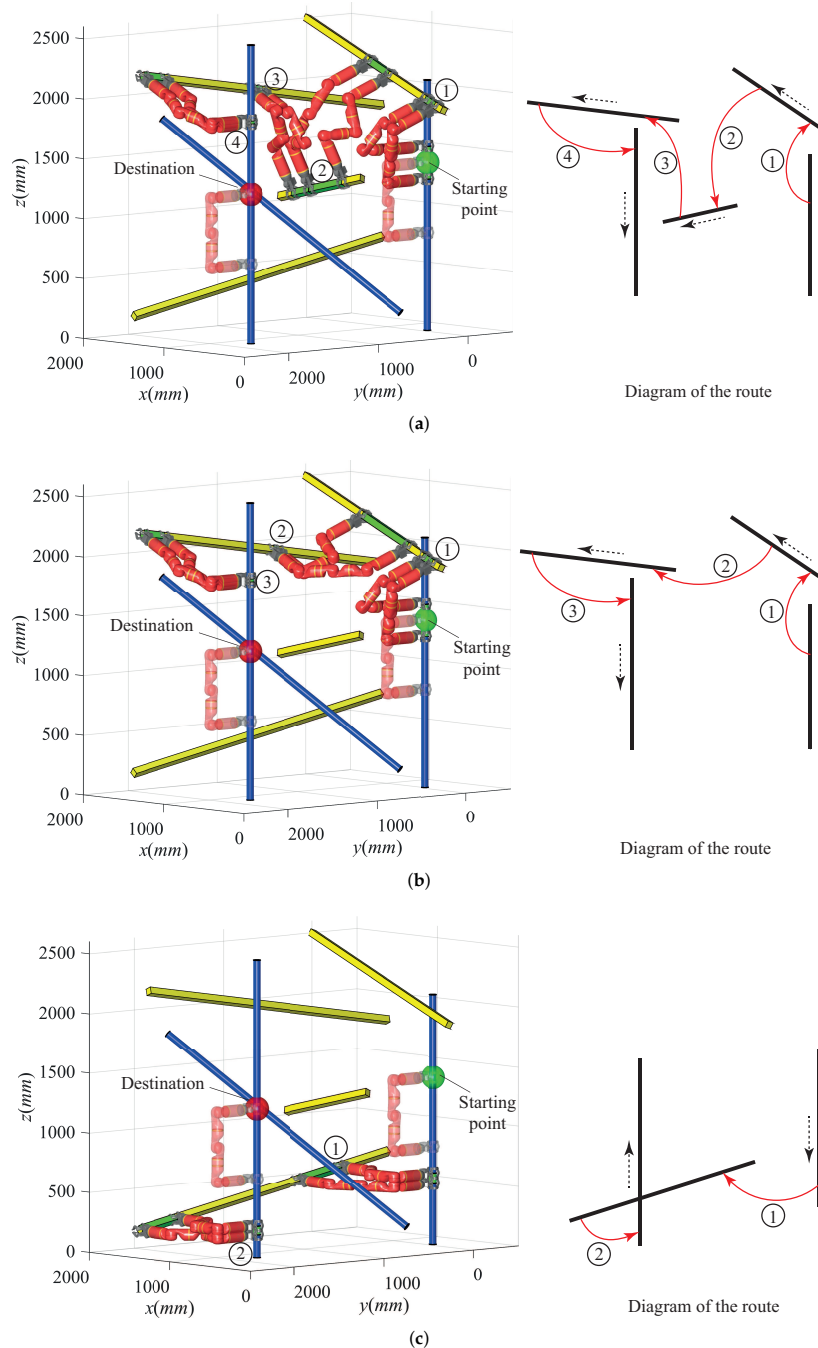


**Figure 9.** Results of global path determination in Scene I consisting of 7 members. (a) Route I; (b) Route II; (c) Route III.

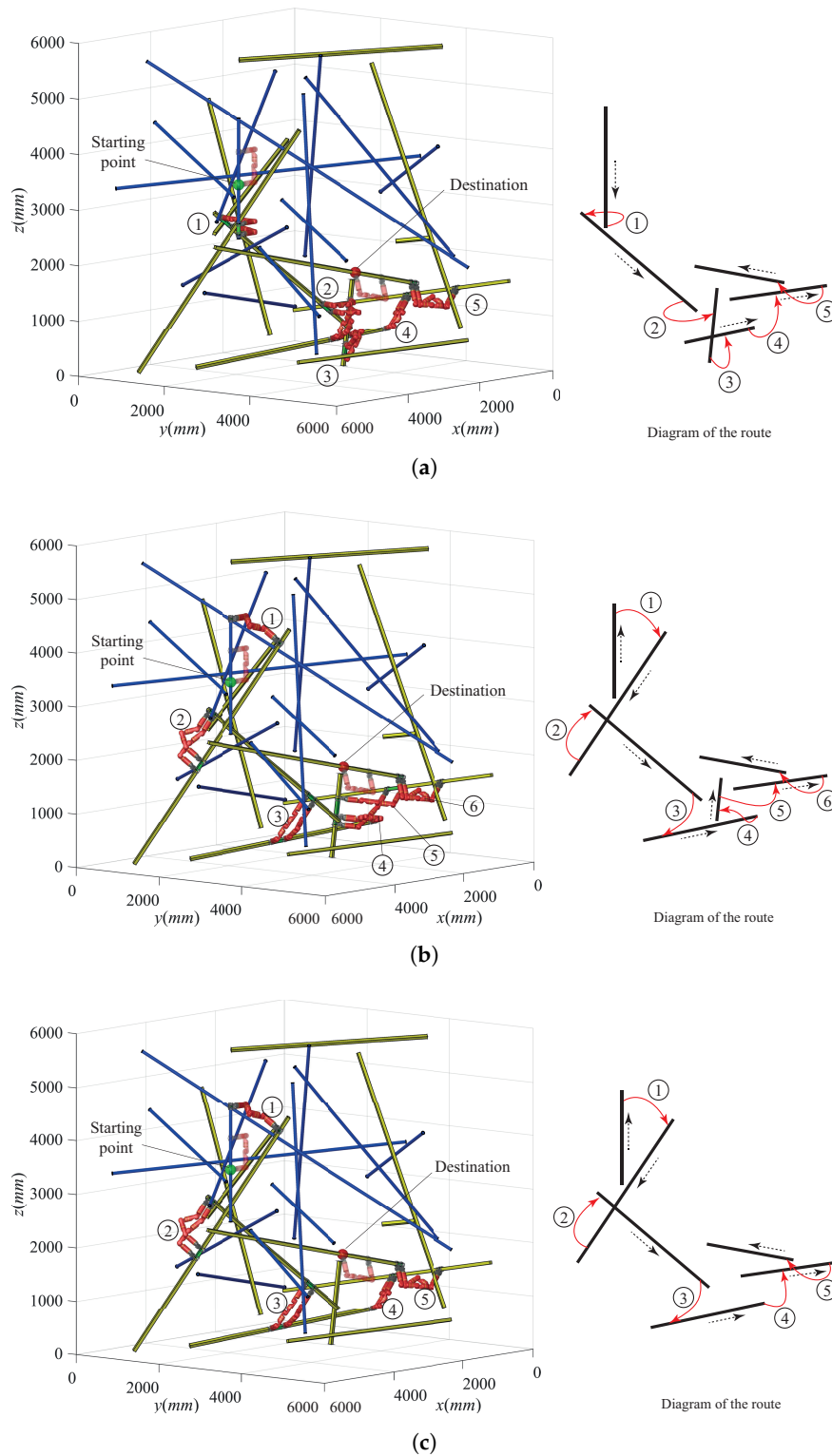


**Figure 10.** Results of global path determination in Scene II consisting of 25 members. (a) Route I; (b) Route II; (c) Route III.

From Figure 9, there are in total three possible routes globally, passing through 3, 2, and 1 in-between members, respectively. Correspondingly, the robot needs to perform 4, 3, and 2 periods of transition. Among the possible routes, Route III shown in Figure 9c is the best solution, regardless of whether the point of transition numbers or the total path length are evaluated. With regard to the

complicated truss scene shown in Figure 10, whose members are randomly generated, the proposed algorithms also determine three possible global routes. From the results, we can see that the robot needs to perform 5 to 6 periods of transition in order to reach the target member. Routes I and III have a superiority in terms of transition number and path length over Route II. However, the routes are not so different from each other. They mainly branch off at the lower right local region where several squared members are concentrated, providing more potential gripping orientations. As a comparison of time consumed, the determination process requires 207.6 ms for the simple case, as compared to 1274.6 ms for the complicated one.

## 6. Conclusions and Future Work

Biped climbing robots represent an ideal automation solution so that human workers do not need to perform high-rise truss-related routine tasks. To freely move in the truss environments, member-to-member transition is a basic and important ability for biped climbing robots.

In this paper, we presented a complete approach to compute the feasibility and corresponding operational regions for transiting from one member to another with biped climbing robots, such as Climbot. The transition analysis takes the safety, reachability, and accessibility of grips in to account. This achievement was then applied to the rapid determination of global paths as a core evaluation for the first time. Simulations successfully verified the effectiveness and efficiency of the presented analysis and algorithms. A novel contribution of this paper is the presentation of a systematic scheme to quantitatively analyze the feasibility of member-to-member transition performed with biped climbing robots. This scheme solves the operational region completely. However, the proposed transition analysis has its own limitation. Owing to the introduction of planar configuration constraints (not usually the case for robots with more than 5 DoF), the transition analysis is only applicable to robots with up to 5 DoF. Another contribution of this paper is a novel path planning algorithm to rapidly determinate feasible global routes for biped climbing robots to move in 3D complex truss environments. This path planning algorithm is greatly beneficial to all the biped climbing robots if their transition capabilities can be modeled and calculated, by outputting global guidance for subsequent planning procedures.

In the near future, we will explore a more general idea for performing transition analysis, which will be applicable to all biped climbing robots. We also plan to propose criteria for the evaluation of the global routes' qualities, and then develop subsequent planners to generate the entire climbing path, i.e., optimal grip sequencer and single-step motion planner. Extensive climbing experiments on various trusses will be conducted to further verify our planning algorithms.

**Acknowledgments:** This research is supported in part by the National Natural Science Foundation of China (Grant Nos. 51605096, 51705086), the NSFC-Guangdong Joint Fund (Grant No. U1401240), the Frontier and Key Technology Innovation Special Funds of Guangdong Province (Grant Nos. 2014B090919002, 2015B010917003, 2015B090922003, 2017B050506008), and the Program of Foshan Innovation Team of Science and Technology (Grant No. 2015IT100072).

**Author Contributions:** Haifei Zhu and Yisheng Guan co-organized the work. Haifei Zhu and Shichao Gu conceived and designed the planner and performed the simulation work. Haifei Zhu wrote the manuscript. Li He analyzed the simulation data, and co-worked with Hong Zhang to prepare the final manuscript. Yisheng Guan and Hong Zhang co-supervised the research.

**Conflicts of Interest:** The authors declare no conflict of interest.

## References

1. Xu, Y.; Brown, B.; Aoki, S.; Kanade, T. Mobility and Manipulation of a Light-weight Space Robot. *Robot. Auton. Syst.* **1994**, *13*, 1–12.
2. Balaguer, C.; Gimenez, A.; Pastor, J.; Padron, V.M. A Climbing Autonomous Robot for Inspection Application in 3D Complex Environments. *Robotica* **2000**, *18*, 287–297.
3. Nakanishi, J.; Fukuda, T.; Koditschek, D.E. A Brachiating Robot Controller. *IEEE Trans. Robot. Autom.* **2000**, *16*, 109–123.

4. Saltaren, R.; Aracil, R.; Reinoso, O.; Scarano, M. Climbing Parallel Robot: A Computational and Experimental Study of its Performance around Structural Nodes. *IEEE Trans. Robot.* **2005**, *21*, 16–22.
5. Aracil, R.; Saltaren, R.; Reinoso, O. A Climbing Parallel Robot: A Robot to Climb along Tubular and Metallic Structures. *IEEE Robot. Autom. Mag.* **2006**, *13*, 16–22.
6. Kushihashi, Y.; Koji, Y.; Yoshikawa, K. Development of Tree-climbing and Pruning Robot WOODY-1: Simplification of Control Using Adjust Function of Grasping Power. In Proceedings of the JSME Conference on Robotics and Mechatronics, Tokyo, Japan, 26–28 May 2006; pp. 1A1-E08\_1–1A1-E08\_2. (In Japanese)
7. Takeuchi, M.; Namba, H.; Suga, Y.; Shirai, Y.; Sugano, S. Development of Street Tree Climbing Robot WOODY-2. In Proceedings of the JSME Conference on Robotics and Mechatronics, Fukuoka, Japan, 24–26 May 2009; pp. 1A2-D07\_1–1A2-D07\_2. (In Japanese)
8. Detweiler, C.; Vona, M.; Yoon, Y.; Yun, S.; Rus, D. Self-assembling Mobile Linkages. *IEEE Robot. Autom. Mag.* **2007**, *14*, 45–55.
9. Spenko, M.J.; Haynes, G.C.; Saunders, J.A.; Cutkosky, M.R.; Rizzi, A.A. Biologically Inspired Climbing with a Hexapedal Robot. *J. Field Robot.* **2008**, *24*, 223–242.
10. Haynes, G.C.; Khripin, A.; Lynch, G.; Amory, J.; Saunders, A.; Rizzi, A.A.; Koditschek, D.E. Rapid Pole Climbing with a Quadrupedal Robot. In Proceedings of the IEEE International Conference on Robotics and Automation, Kobe, Japan, 12–17 May 2009; pp. 2767–2772.
11. Noohi, E.; Mahdavi, S.; Baghani, A.; Nili-Ahmadabadi, M. Wheel-Based Climbing Robot: Modeling and Control. *Adv. Robot.* **2010**, *24*, 1313–1343.
12. Tavakoli, M.; Marques, L.; Almeida, A. Development of an Industrial Pipeline Inspection Robot. *Ind. Robot Int. J.* **2010**, *37*, 309–322.
13. Lam, T.L.; Xu, Y. A Flexible Tree Climbing Robot: Treebot—Design and Implementation. In Proceedings of the IEEE International Conference on Robotics and Automation, Shanghai, China, 9–13 May 2011; pp. 5849–5854.
14. Vidoni, R.; Mimmo, T.; Pandolfi, C. Tendril-Based Climbing Plants to Model, Simulate and Create Bio-Inspired Robotic Systems. *J. Bionic Eng.* **2015**, *12*, 250–262.
15. Guan, Y.; Jiang, L.; Zhang, X. Mechanical Design and Basic Analysis of a Modular Robot with Special Climbing and Manipulation Functions. In Proceedings of the IEEE International Conference on Robotics and Biomimetics, Sanya, China, 15–18 December 2007; pp. 502–507.
16. Guan, Y.; Jiang, L.; Zhu, H.; Zhou, X.; Cai, C.; Wu, W.; Xiao, Z.; Chen, X.; Zhang, H. Climbot: A Bio-inspired Modular Biped Climbing Robot—System Development, Climbing Gaits and Experiments. *ASME J. Mech. Robot.* **2016**, *8*, 021026.
17. Rollinson, D.; Choset, H. Pipe Network Locomotion with a Snake Robot. *J. Field Robot.* **2016**, *33*, 322–336.
18. Balaguer, C.; Gimenez, A.; Jardon, A. Climbing Robots' Mobility for Inspection and Maintenance of 3D Complex Environments. *Auton. Robot.* **2005**, *18*, 157–169.
19. Chu, B.; Jung, K.; Han, C.S.; Hong, D. A Survey of Climbing Robots: Locomotion and Adhesion. *Int. J. Precis. Eng. Manuf.* **2010**, *11*, 633–647.
20. Muscolo, G.G.; Recchiuto, C.T.; Sellers, W.; Molfino, R. Towards a Novel Embodied Robot Bio-inspired by Non-human Primates. In Proceedings of the 41st International Symposium on Robotics/Robotik 2014, Munich, Germany, 2–3 June 2014; pp. 1–7.
21. Tummala, R.L.; Mukherjee, R.; Xi, N.; Aslam, D.; Dulimarta, H.; Xiao, J.; Minor, M.; Dang, G. Climbing the Walls—Presenting Two Underactuated Kinematic Designs for Miniature Climbing Robots. *IEEE Robot. Autom. Mag.* **2002**, *9*, 10–19.
22. Balaguer, C.; Gimenez, A.; Huete, A.J.; Sabatini, A.M.; Topping, M.; Bolmsjo, G. The MATS Robot: Service Climbing Robot for Personal Assistance. *IEEE Robot. Autom. Mag.* **2006**, *13*, 51–58.
23. Chung, W.; Xu, Y. A Novel Frame Climbing robot: Frambot. In Proceedings of the IEEE International Conference on Robotics and Biomimetics, Phuket, Thailand, 7–11 December 2011; pp. 2559–2566.
24. Guan, Y.; Zhu, H.; Wu, W.; Zhou, X.; Jiang, L.; Cai, C.; Zhang, L.; Zhang, H. A Modular Biped Wall-Climbing Robot with High Mobility and Manipulating Function. *IEEE/ASME Trans. Mechatron.* **2013**, *18*, 1787–1798.
25. Silva, M.F.; Machado, J.A.T. A Survey of Technologies and Applications for Climbing Robots Locomotion and Adhesion. In *Climbing and Walking Robots*; InTech: London, UK, 2010; pp. 1–22.
26. Schmidt, D.; Berns, K. Climbing Robots for Maintenance and Inspections of Vertical Structures—A Survey of Design Aspects and Technologies. *Robot. Auton. Syst.* **2013**, *61*, 1288–1305.

27. Yoon, Y.; Rus, D. Shady3D: A Robot that Climbs 3D Trusses. In Proceedings of the IEEE International Conference on Robotics and Automation, Roma, Italy, 10–14 April 2007; pp. 4071–4076.
28. Chung, W.; Xu, Y. Minimum Energy Demand Locomotion on Space Station. *J. Robot.* **2013**, *2013*, 723535.
29. Cai, C.; Zhu, H.; Guan, Y.; Zhang, X.; Zhang, H. A Biologically Inspired Miniature Biped Climbing Robot. In Proceedings of the IEEE International Conference on Mechatronics and Automation, Changchun, China, 9–12 August 2009; pp. 2653–2658.
30. Cai, C.; Guan, Y.; Zhou, X.; Jiang, L.; Zhu, H.; Wu, W.; Zhang, X.; Zhang, H. Joystick-based Control for a Biomimetic Biped Climbing Robot. *Robot* **2012**, *34*, 363–368. (In Chinese)
31. Zhu, H.; Guan, Y.; Wu, W.; Chen, X.; Zhou, X.; Zhang, H. A Binary Approximating Method for Graspable Region Determination of Biped Climbing Robots. *Adv. Robot.* **2014**, *28*, 1405–1418.
32. Xu, Y.; Brown, B.; Kanade, T. Control Systems of the Self-Mobile Space Manipulator. *IEEE Trans. Control Syst. Technol.* **1994**, *2*, 207–219.
33. Yun, S.; Rus, D. Optimal Self Assembling of Modular Manipulators with Active and Passive Modules. *Auton. Robot.* **2011**, *31*, 183–207.
34. Lam, T.; Xu, Y. Motion Planning for Tree Climbing with Inchworm-like Robots. *J. Field Robot.* **2013**, *30*, 87–101.
35. Zhu, H.; Guan, Y.; Wu, W.; Zhou, X.; Zhang, H. Transition Analysis of a Biped Pole-Climbing Robot—Climbot. In Proceedings of the 16th International Conference on Climbing and Walking Robots, Sydney, Australia, 14–17 July 2012; pp. 685–692.



© 2018 by the authors. Licensee MDPI, Basel, Switzerland. This article is an open access article distributed under the terms and conditions of the Creative Commons Attribution (CC BY) license (<http://creativecommons.org/licenses/by/4.0/>).